

Simultaneous catalytic regime of tritium and helium-3 in D–D fusion without external breeding

M MAHDAVI* and T KOOHROKHI

Physics Department, Mazandaran University, P.O. Box 47415-416, Babolsar, Iran

*Corresponding author. E-mail: m.mahdavi@umz.ac.ir

MS received 27 May 2009; revised 26 September 2009; accepted 20 October 2009

Abstract. A catalytic regime of tritium and helium-3 in deuterium–deuterium fusion, including ion–electron collisions, mechanical expansion, bremsstrahlung radiation, inverse Compton scattering losses and reacting particles energy effect has been investigated. In this paper a new fuel configuration, $DT_x\ ^3\text{He}_y$, is formed by adding ^3He to DT fuel. According to our calculations this fuel ($DT_{x=0.0112}\ ^3\text{He}_{y=0.0399}$) has greater energy gain than the fuel ($DT_{x=0.0112}$) used by Eliezer *et al* [Eliezer *et al*, *Nucl. Fusion* **40**, 195 (2000)] and also it does not require external tritium and helium-3 breeding. Furthermore, neutron yields in D–D and D–T reactions are reduced due to the reduced quantity of initial amount of deuterium and tritium.

Keywords. Fusion fuel pellet; energy gain; internal breeding; inverse Compton scattering; neutron generation.

PACS Nos 25.60.Pj; 52.40.Mj; 52.50.-b

1. Introduction

Advanced fusion fuels are very appealing from the point of view of radiological cleanness, but they are very difficult to exploit because of their ultrahigh ignition temperatures [1–4]. Theoretical analysis has demonstrated that it will not be possible to use the neutronless fusion cycles in stoichiometric plasmas because of radiation losses and burn-up effects [5,6].

It has been demonstrated that adding a small amount of tritium can reduce the ignition temperature of deuterium and advanced fuel inertial fusion targets [7–10]. Since external generation of tritium has several problems, the possibility of a catalytic regime for tritium, where the need for external tritium breeding is avoided, is very important. It has recently been shown that internal tritium breeding takes place as the fusion pellet burns up and a small amount of tritium added to a deuterium plasma enables triggering of ignition at less than 10 keV [11].

In the D– ^3He reaction, the generated charged particles eliminate most of the energetic neutron generation in D–T reaction. Moreover, the reaction rate of this

reaction is larger than D–D reactions in the temperature interval $25 \text{ keV} < T < 250 \text{ keV}$. However, ^3He is not abundant in Earth. It has been pointed out that it can be mined from Moon [12] or from Jupiter [13] but developing the required technology for non-terrestrial mining presents a daunting task. So, internal breeding of helium-3 as well as tritium is very important in fusion fuel pellet design.

A high density scenario, i.e. a typical pellet of inertial confinement fusion, has been chosen for this analysis [14–16]. It is presumed that a pellet of a given fuel has been compressed up to a required density and areal density. The mechanical disassembly of the pellet is taken into account by presuming that the plasma is a sphere whose radius expands at the speed of sound inside the plasma. Therefore, the energy gains computed in this article only refer to the energy generated in the originally heated plasma, without taking into account the fact that much more energy would be generated if fusion ignition were propagated to the surrounding cold fuel. Thus, the gain for a spark ignition scheme would be much higher than the one calculated in this article.

The simulation model is introduced in §2. In the next three subsections energy deposition of charged particles and neutrons, the inverse Compton effect and effect of reacting particles' energy in fuel pellet parameters, are discussed respectively. Results and discussions are given in §3 and finally conclusion is given in §4.

2. The simulation model

The simulation model used by Eliezer *et al* [11] is as follows: thermonuclear reaction starts in a DT fusion pellet of $2.5 \times 10^{-3} \text{ cm}$ radius which has been compressed to a density of 5000 g/cm^3 at a temperature of 10 keV . The following reactions occur predominantly:



The neutron and proton channels of the D–D reaction occur with 50% probability. N_k , the total number of particles of species k , is governed by the equation

$$\frac{dN_k}{dt} = \sum_{j=1}^4 a_k^j N_{j(1)} N_{j(2)} \langle \sigma v \rangle_j \frac{1}{V}, \quad (5)$$

where V is the volume of the heated plasma, $\langle \sigma v \rangle_j$ is the Maxwell averaged reaction rate of reaction j and a_k^j is the number of particles of species k formed or destroyed in the reaction j . We use the more accurate fits formula for the Maxwell averaged

reaction rates [17]. Six species are considered in this calculation: D, ^3He , T, p, ^4He and n. The equation of energy balance for ions and electrons are given by

$$\frac{3}{2} \frac{d}{dt}(N_i T_i) = \sum_{j=1}^4 \sum_{k=1}^6 f_k^j w_k^j E_j N_{j(1)} N_{j(2)} \langle \sigma v \rangle_j \frac{1}{V} - \frac{P_{ie}}{V} - N_i T_i 4\pi R^2(t) C_s \frac{1}{V}, \quad (6)$$

$$\frac{3}{2} \frac{d}{dt}(N_e T_e) = \sum_{j=1}^4 \sum_{k=2}^6 (1 - f_k^j) w_k^j E_j N_{j(1)} N_{j(2)} \langle \sigma v \rangle_j \frac{1}{V} + \frac{P_{ie}}{V} - \frac{P_B}{V} - P_C - N_e T_e 4\pi R^2(t) C_s \frac{1}{V}, \quad (7)$$

where T_i is the ion temperature, E_j is the energy yield of reaction j , w_k^j is the fraction of E_j carried by the product k , f_k^j is the fraction of the energy of the product k created in the reaction j that is deposited into the plasma ions, $R(t)$ is the pellet radius, C_s is the speed of sound and T_e , P_B and P_C are electron temperature, bremsstrahlung term and inverse Compton scattering term, respectively.

The total number of ions

$$N_i = \sum_{k=2}^6 N_k, \quad (8)$$

where k varies from 2 to 6 as $k = 1$ stands for neutrons.

P_{ie} is the ion–electron energy exchange term that is achieved by

$$P_{ie} \left(\frac{\text{keV cm}^3}{\text{s}} \right) = 1.69 \times 10^{-13} N_e \sum_{k=2}^6 \ln \Lambda_{ek} Z_k^2 \frac{N_k}{m_k} \times \frac{T_i - T_e}{T_e^{1/2}}, \quad (9)$$

where m_k and Z_k are the mass number and the charge of nuclei k , respectively. The Coulomb logarithm for ion–electron collision is [18],

$$\ln \Lambda_{ek} = 23 - \ln \left[\left(\frac{N_e}{V} \right)^{0.5} Z_k T_e^{-1.5} (\text{eV}) \right]. \quad (10)$$

The bremsstrahlung loss, P_B , is given by

$$P_B \left(\frac{\text{keV cm}^3}{\text{s}} \right) = 2.94 \times 10^{-15} N_e \sum_{k=2}^6 N_k Z_k^2 T_e^{0.5} \times \left(1 + \frac{2T_e}{511.1} \right), \quad (11)$$

where $2T_e$ (keV)/511.1 is a relativistic correction term. In the mechanical expansion term, the speed of sound is computed using

$$C_s = \sqrt{\frac{\gamma P}{\rho}}, \quad (12)$$

where ρ is the density, $\gamma = \frac{5}{3}$ and P is the total pressure,

$$P = \frac{1}{V}(N_e T_e + N_i T_i). \quad (13)$$

The radius of the pellet is governed by

$$R(t) = R(t - \Delta t) + \phi C_s \Delta t, \quad (14)$$

where $C_s \Delta t$ is the effective outer radius speed which simulates the stagnation phase after the implosion of the pellet, such that

$$\phi = \begin{cases} \phi(t), & \phi(t) < \phi_0 \\ 1, & \phi(t) \geq \phi_0, \end{cases} \quad (15)$$

where $\phi(t) = 1 - N_D(t)/N_D(0)$ is the burn-up fraction and $\phi_0 = 0.5$, in accordance with pellet performance simulations [19–21].

The energy gain is defined as the ratio between the total energy created by the fusion reactions,

$$E_{\text{fus}}^{\text{tot}} = \int_0^\infty dt \sum_{j=1}^4 E_j N_{j(1)} N_{j(2)} \langle \sigma v \rangle_j \frac{1}{V} \quad (16)$$

and the energy contained in the originally heated plasma,

$$E_{\text{input}} = \frac{3}{2}(N_e(0)T_e(0) + N_i(0)T_i(0)), \quad (17)$$

i.e.

$$\text{GAIN} = \frac{E_{\text{fus}}^{\text{tot}}}{E_{\text{input}}}. \quad (18)$$

The catalytic regime of tritium is obtained when the final amount of tritium is slightly higher than the initial amount. In this case, external tritium breeding is avoided, and is replaced by internal tritium breeding. The internal tritium breeding (ITB) is defined as

$$\text{ITB} = \frac{N_T(t = \infty)}{N_T(t = 0)}. \quad (19)$$

It is worthwhile noting here, as we have discussed in §1, the value of y to be obtained so that internal helium-3 breeding (IHB) is to occur. For this aim, we shall define a new parameter that determines internal helium-3 breeding:

$$\text{IHB} = \frac{N_{3\text{He}}(t = \infty)}{N_{3\text{He}}(t = 0)}. \quad (20)$$

2.1 *Energy deposition of charged particles and neutrons*

For low-density and high-temperature plasmas, Coulomb interactions can be approximated as small-angle binary collisions [22]. However, large-angle Coulomb scattering and collective plasma effects need to be included for high densities [23]. Li and Petrasso [24] obtained the energy loss of charged particles per unit length in a typical ICF fusion fuel pellet by considering these effects. According to their calculations, the energy loss of the projectile p with mass m_p to the plasma particles of species b with mass m_b or, equivalently, the energy gain of the plasma particles b brought about by the projectile p moving through the plasma with velocity v_p , is defined as

$$\left(\frac{dE_p}{dx}\right)_b = \frac{Z_p^2 e^2}{v_p^2} \frac{k_b^2}{\beta_b m_b} \left[G\left(\frac{1}{2}\beta_b m_b v_p^2\right) \ln \Lambda_b + H\left(\frac{1}{2}\beta_b m_b v_p^2\right) \right], \quad (21)$$

where $T_b = \beta_b^{-1}$ is the temperature of plasma species b measured in energy units, $Z_p e$ is the charge of the projectile whose energy loss is being considered, $Z_b e$ is the charge of a plasma species labelled by b , and k_b is the Debye wave number of these species, which has density n_b , so that

$$k_b^2 = 4\pi\beta_b Z_b e n_b. \quad (22)$$

The total Debye wave number of the plasma is given by the sum over all the species,

$$k_D^2 = \sum_b k_b^2. \quad (23)$$

Here

$$G(y) = \left[1 - \frac{m_b}{m_p} \frac{d}{dy} \right] \mu(y), \quad (24)$$

where

$$\mu(y) = \frac{2}{\sqrt{\pi}} \int_0^y dz z^{1/2} e^{-z} \quad (25)$$

and

$$H(y) = \frac{m_b}{m_p} \left[1 + \frac{d}{dy} \right] + \theta(y-1) \ln \left(2e^{-\gamma} y^{1/2} \right) \quad (26)$$

with $\theta(x)$ the unit step function: $\theta(x) = 0$ for $x < 0$ and $\theta(x) = 1$ for $x > 0$. Li and Petrasso defined a Coulomb logarithm in terms of the combination of classical and quantum cut-offs as described above, namely

$$\ln \Lambda_b = -\frac{1}{2} \ln k_D^2 B_b^2, \quad (27)$$

where

$$B_b^2 = \left(\frac{\hbar}{2m_{pb}u_b} \right)^2 + \left(\frac{Z_p Z_b e^2}{m_{pb}u_b} \right)^2 \quad (28)$$

in which m_{pb} is the reduced mass of the projectile (p)-plasma particle (b) system,

$$\frac{1}{m_{pb}} = \frac{1}{m_p} + \frac{1}{m_b} \quad (29)$$

and

$$u_b^2 = v_p^2 + \frac{2}{\beta_b m_b} \quad (30)$$

defines an average of the squared projectile and thermal velocities.

By using eq. (21) we can now calculate the fraction of energy deposited to ions,

$$f_k^j = \frac{1}{w_k^j E_j - \frac{3}{2} T_i} \int_{\frac{3}{2} T_i}^{w_k^j E_j} \frac{(dE/dx)_i}{(dE/dx)_e + (dE/dx)_i} dE. \quad (31)$$

The fraction of neutron energy deposited in the plasma, as used by Eliezer *et al* [9], (a) for 14.1 MeV neutrons is,

$$f_n = \frac{\rho R}{\rho R + 13.72},$$

and (b) for 2.45 MeV neutrons,

$$f_n = \frac{\rho R}{\rho R + 3.92}.$$

2.2 The inverse Compton effect

At high electron temperatures, the electron energy loss by the inverse Compton effect might be important to both the internal tritium breeding ratio and the pellet gain. Gsponer and Hurni suggested that the three-temperature Hurwitz model can be used to calculate the radiation temperature evolution due to bremsstrahlung and Compton effects [25,26]. The main assumption of this model is that for any electron temperature, all the created bremsstrahlung radiation will become Planckian. This assumption might be reasonable for optically thick plasma, but is unjustified for the optically thin plasma. For the optically thick plasma, the mean free path of bremsstrahlung photons is smaller than the plasma radius and radiation can be treated as a photon gas in thermal equilibrium. Thus, a black body radiation spectrum is obtained and the radiation temperature can be defined. In this case, the inverse Compton effect can significantly reduce the electron temperature and increase accordingly the radiation temperature. However, in the limit of optically thin plasma, radiation created by bremsstrahlung is unlikely to become Planckian.

For the optically thin plasma, the photon spectrum will be determined by the bremsstrahlung emission spectrum. Thermal equilibration of photons and electrons

does not take place, since hot photons are leaving the plasma before the equilibrium is established. Therefore, for the cases considered here, the three-temperature model is not realistic and will greatly overestimate radiation losses due to the inverse Compton effect. An accurate treatment of the inverse Compton effect can be obtained by using a radiation transport model which would span the optically thick to optically thin plasma transition. Such a model, however, would involve a solution of complicated equations of radiation transport [27–29], which is out of the scope of this article. To estimate the radiation losses due to the inverse Compton effect without fully solving the complicated problem of radiation transport, a simple model based on the optically thin limit is adopted by Eliezer *et al* [11]. Nevertheless, we will also see that their model is accurate for the optically thick plasma in the early stages of the microexplosions, because the electron and radiation temperatures are very similar then.

In the optically thin plasma limit, the total radiation energy density, E_r , can be estimated in terms of the bremsstrahlung loss rate, P_B , if one assumes that the average travelling time of the bremsstrahlung photons through a thin plasma of radius R is $\Delta t \approx R/c$. Then,

$$E_r = \frac{P_B R}{V^2 c}, \quad (32)$$

where c is the speed of light in vacuum. The bremsstrahlung emission spectrum is given by [30]

$$J_\nu(\text{keV}/\text{cm}^3) = 1.25 \times 10^{-32} Z^2 n_e n_i \frac{1}{T_e^{0.5}} e^{-h\nu/kT_e}, \quad (33)$$

where $n_e = N_e/V$ and $n_i = N_i/V$. Using the same approximation as in eq. (32) we define the bremsstrahlung radiation energy density as

$$E^{\text{Br}}(\nu) = J_\nu \frac{R}{c}. \quad (34)$$

We would like to compare this radiation energy density with the radiation energy density of a black body given by

$$E^{\text{BB}}(\nu) = \frac{8\pi}{c^3 h^2} \frac{(h\nu)^3}{e^{h\nu/kT_r} - 1}, \quad (35)$$

where T_r is the radiation temperature. For the black body radiation, the total radiation energy density is

$$E_r(\text{keV}/\text{cm}^3) = \frac{4\sigma}{c} T_r^4, \quad (36)$$

where σ is the Stefan–Boltzmann constant. For the inverse Compton effect, the radiation energy density of hot photons with $h\nu > T_e$ is important,

$$E^{\text{IC}} = \int_{h\nu > T_e}^{\infty} E(\nu) d\nu. \quad (37)$$

In figure 1 we compare the number of photons with $h\nu > T_e$ obtained from the bremsstrahlung radiation spectrum (eq. (34)) and the black body radiation spectrum (eq. (35)) as a function of the electron temperature. As one can see from figure 1, for $T_e < 96.95$ keV the black body radiation spectrum overestimates the number of hot photons. For $T_e > 96.95$ keV, however, the number of hot photons in the bremsstrahlung spectrum is larger than that in the black body radiation spectrum. To estimate the radiation losses due to the inverse Compton effect in the optically thin plasma limit we define the instantaneous radiation temperature, T_r , of bremsstrahlung photons in terms of E_r by equating eqs (32) and (34). The system defined in this way has the same radiation energy as that created by the bremsstrahlung emission, but with a Planckian distribution. Clearly, this assumption is not correct for the optically thin plasma. In fact, in the framework of this approximation, for $T_e < 96.95$ keV, the electron energy losses due to the inverse Compton scattering are overestimated since in this electron temperature range the number of hot photons in the black body spectrum is larger than that in the bremsstrahlung spectrum. Therefore, model by Eliezer *et al* can provide an upper limit for the electron energy losses due to the inverse Compton scattering in an optically thin plasma with relatively low electron temperatures. For $T_e > 96.95$ keV the black body distribution underestimates the number of hot photons. However, we assume that for such high electron temperatures only a fraction of the total number of photons are in instantaneous equilibrium with a temperature T_r ,

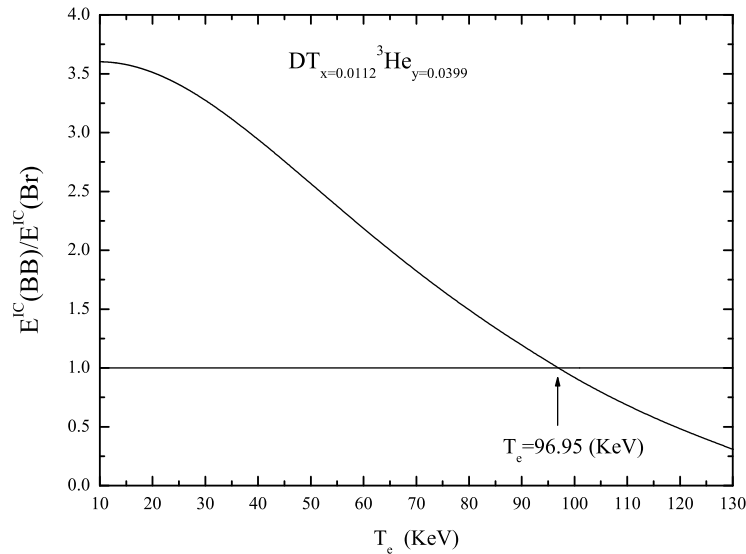


Figure 1. The ratio between the number of hot photons with $h\nu > T_e$ (eq. (37)) obtained from bremsstrahlung radiation spectrum (eq. (34)) and from the black body radiation spectrum (eq. (35)). An areal density $\rho_0 R_0 = 12.5$ g/cm², a density $\rho_0 = 5000$ g/cm³, a ratio of tritium to deuterium particle numbers $x = 0.0112$ and a ratio of helium-3 to deuterium particle numbers $y = 0.0399$ in the initial pellet, was used for this computation.

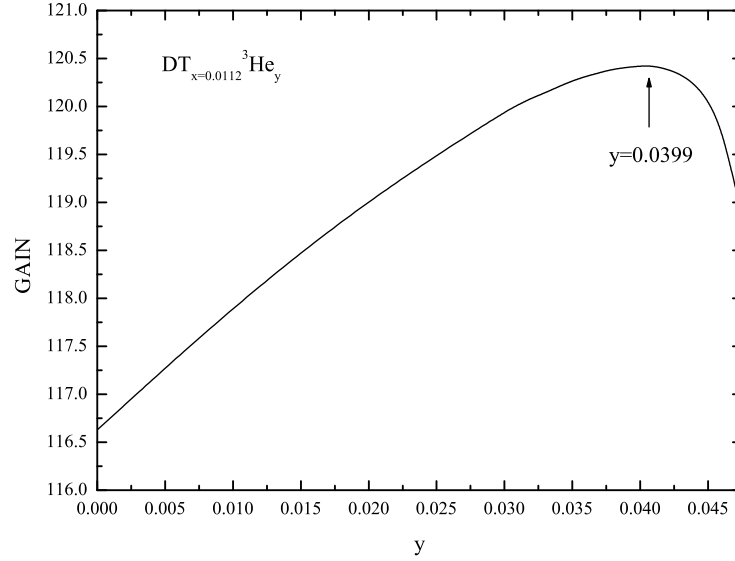


Figure 2. Energy gain vs. ratio of the helium-3 to deuterium particle number in the initial pellet $D-T_{x=0.0112}^3He_y$. The areal density of the initial pellet $\rho_0 R_0 = 12.5 \text{ g/cm}^2$ and the initial temperature of ions and electrons are $T_i(0) = T_e(0) = 10 \text{ keV}$.

whereas the rest is leaving the plasma without having a chance to be scattered by electrons. This fraction is given by the Planck distribution and it becomes smaller as the electron temperature rises. From the Planck distribution for the photons we can easily estimate the inverse Compton scattering contribution. Provided the photons are of low energy, $h\nu/m_e c^2 \ll 1$, and the electron temperature moderate, $kT_e/m_e c^2 \ll 1$, the energy lost by the electrons in inverse Compton scattering is given by ref. [31] as

$$P_C \text{ (keV/s)} = 4E_r N_e c \left(\frac{8}{3} \pi r_e^2 \right) \left(\frac{T_e \text{ (keV)} - T_r \text{ (keV)}}{511.1} \right), \quad (38)$$

where $\frac{8}{3} \pi r_e^2$ is the Thomson cross-section and r_e is the classical electron radius. From eq. (38) it follows that the electron-photon energy exchange grows as the difference between the electron and photon temperatures increases. This is compensated, however, by a small radiation energy density that, in this model, is proportional to the bremsstrahlung radiation rate. In addition, the instantaneous radiation temperature is kept low because most of the photons leave the system without interaction in an optically thin plasma. Although this simplified model is based on the optically thin plasma limit, using eqs (11), (32) and (36) one can verify that for the typical initial parameters used in this article, $\rho R = 12.5 \text{ g/cm}^2$, $\rho = 5000 \text{ g/cm}^3$ and $T_e = 10 \text{ keV}$ (for which the plasma is optically thick), the radiation temperature is about equal to the electron temperature. For an optically thick plasma, this can be understood by assuming a time-independent thermal equilibrium between the bremsstrahlung source and the black body losses,

$$\frac{P_B}{V} = \sigma T_r^4 4\pi R^2. \tag{39}$$

This equation yields a value of T_r equal to the one derived by eqs (32) and (36) up to a factor of $(4/3)^{1/4} = 1.07$. Therefore, this model gives a satisfactory approximation to the initial conditions of an optically thick plasma.

2.3 Effect of reacting particles' energy in fuel pellet parameters

For most fusion reactions, from controlled fusion reactors to solar processes, the reacting particles have energies in the range of 1–10 keV. The initial kinetic energies are thus small compared to the Q values of several MeV. The energy released and the final total energy of the product particles will then be equal to the Q value. But, as we shall show (figure 5), when fuel pellet is burning up, its temperature will reach about 200 keV, or even higher. If we assume that incoming particles have kinetic energy equivalent to this temperature ($2\frac{3}{2}kT = 600$ keV), the ratio of this energy to the Q value, i.e. one of D–D reaction channels, is $600/3256 = 0.18$. Thus, as we shall find, application of this energy will affect the fuel parameters.

We now recalculate E_j , the energy yield in reaction j . Throughout this work, we assume that reacting particles moving together and incoming to the reaction with energy equivalent to the ion temperature in the fuel pellet. Therefore, E_j is given by

$$E_j = T_0^{c.m.} + Q_j, \tag{40}$$

where $T_0^{c.m.}$ is the total kinetic energy of the reacting particles in the centre of mass coordinate. This quantity is related to its value in laboratory coordinate as

$$T_0^{lab} = T_0^{c.m.} + T_{c.m.}, \tag{41}$$

where $T_{c.m.}$ is the centre of mass kinetic energy of the system that is equal to

$$T_{c.m.} = \frac{1}{2} M_{c.m.} V_{c.m.}^2 = \frac{1}{2} (m_1 + m_2) \left(\frac{m_2 u_2 - m_1 u_1}{m_1 + m_2} \right)^2, \tag{42}$$

where u_1 and u_2 are the velocities, and m_1 and m_2 are the masses of reacting particles 1 and 2, respectively. In this equation we assume that $m_2 > m_1$. As we know $T_1 = \frac{3}{2}T_i = \frac{1}{2}m_1u_1^2$ and $T_2 = \frac{3}{2}T_i = \frac{1}{2}m_2u_2^2$ that T_1 and T_2 are the kinetic energies of reacting particles and T_i is the ion temperature that we have assumed to be the same for all ions in the plasma. Thus we can rewrite this equation as

$$T_{c.m.} = \frac{3}{2}T_i - 2\frac{3}{2}T_i \left(\frac{\sqrt{m_1 m_2}}{m_1 + m_2} \right). \tag{43}$$

The total kinetic energy of the reacting particles is also in laboratory coordinate as

$$T_0^{lab} = T_1 + T_2 = 2 \left(\frac{3}{2}T_i \right). \tag{44}$$

Then using eqs (44), (43) and (41) we have

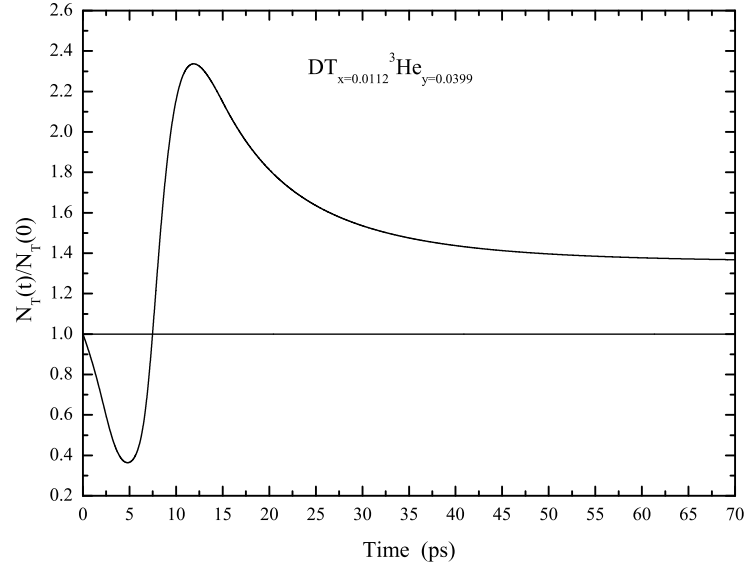


Figure 3. Ratio of the number of tritium particles at time t and the initial number of tritium particles as a function of burning time. The initial tritium to deuterium ratio $x = 0.0112$. The initial helium-3 to deuterium ratio $y = 0.0399$. The density of the initial pellet $\rho_0 = 5000 \text{ g/cm}^3$. The areal density $\rho_0 R_0 = 12.5 \text{ g/cm}^2$ and the initial temperature of ions and electrons are $T_i(0) = T_e(0) = 10 \text{ keV}$.

$$T_0^{\text{c.m.}} = \frac{3}{2} T_i \frac{(\sqrt{m_1} + \sqrt{m_2})^2}{m_1 + m_2}. \quad (45)$$

And finally by substituting this equation in eq. (40) we obtain,

$$E_j = \frac{3}{2} T_i \frac{(\sqrt{m_{j(1)}} + \sqrt{m_{j(2)}})^2}{m_{j(1)} + m_{j(2)}} + Q_j. \quad (46)$$

This equation shows that energy yield in reaction j is proportional to the ion temperature, mass of the reacting particles ($m_{j(1)}$ and $m_{j(2)}$) and Q_j value of reaction. While the last two quantities are time independent, ion temperature of fuel pellet varies with time. Therefore, using these calculations, E_j is a time-dependent quantity.

3. Results and discussions

We consider an optimal pellet configuration of density $\rho_0 = 5000 \text{ g/cm}^3$, $\rho_0 R_0 = 12.5 \text{ g/cm}^2$ (R is the pellet radius), and initial ion, electron temperatures given by $T_i = T_e = 10 \text{ keV}$, analysed by Eliezer *et al.* This analysis showed that the tritium breeding takes place when tritium fraction $x = 0.0112$. The increase in the initial ratio of tritium x leads to an increase in energy gain and a decrease in

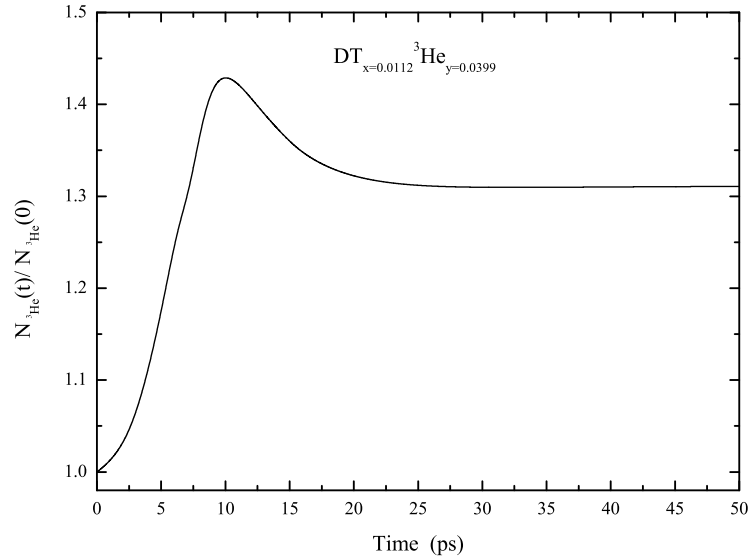


Figure 4. Ratio of the number of helium-3 particles at time t and the initial number of helium-3 particles as a function of burning time. The initial tritium to deuterium ratio $x = 0.0112$. The initial helium-3 to deuterium ratio $y = 0.0399$. The density of the initial pellet $\rho_0 = 5000 \text{ g/cm}^3$. The areal density $\rho_0 R_0 = 12.5 \text{ g/cm}^2$, and the initial temperature of ions and electrons are $T_i(0) = T_e(0) = 10 \text{ keV}$.

ignition temperature, but this increases destroyer effects due to energetic neutron generation yield in D–T reaction. To recover some of the energy gain that is decreased with the reduction in the initial ratio of tritium, we add a small amount of ^3He in the fuel pellet DT_x . For this purpose, we consider fuel pellet in the new form $\text{DT}_x\ ^3\text{He}_y$ where y is the ratio of helium-3 to deuterium, and x is the

Table 1. Maximum ion, electron and radiation temperatures (in keV), burn fraction, generated final neutron particle number, tritium and helium-3 breeding ratio in the $\text{D-T}_{x=0.0112}\ ^3\text{He}_{y=0.0399}$ and $\text{D-T}_{x=0.0112}$ fuel pellet.

In $\text{D-T}_{x=0.0112}\ ^3\text{He}_{y=0.0399}$ fuel pellet discussed in this article	In $\text{D-T}_{x=0.0112}$ fuel pellet as suggested by Eliezer <i>et al</i> [11]
$T_i^{\text{max}} = 255.7 \text{ keV}$	$T_i^{\text{max}} = 240.7 \text{ keV}$
$T_e^{\text{max}} = 137.2 \text{ keV}$	$T_e^{\text{max}} = 128.4 \text{ keV}$
$T_r^{\text{max}} = 18.2 \text{ keV}$	$T_r^{\text{max}} = 17.5 \text{ keV}$
GAIN = 120.7	GAIN = 116.9
Burn fraction = 0.59	Burn fraction = 0.54
$N_n^{\text{final}} = 164 \times 10^{17}$	$N_n^{\text{final}} = 185 \times 10^{17}$
ITB = 1.36	ITB = 1.28
IHB = 1.31	

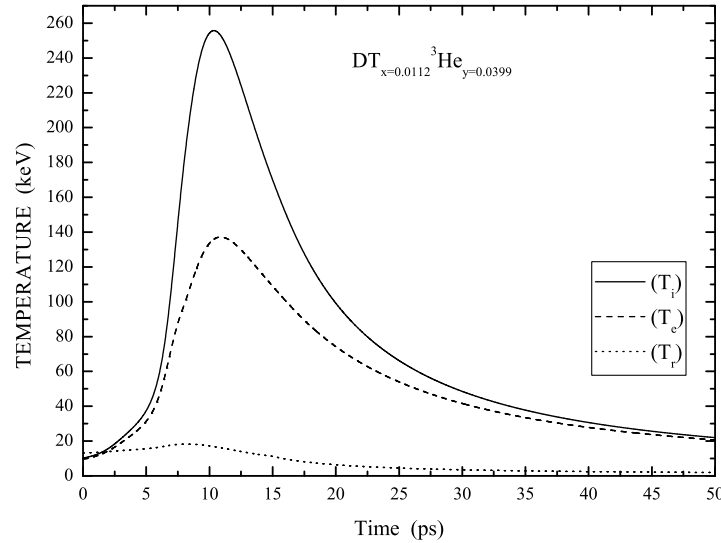


Figure 5. Ion, electron and radiation temperatures as a function of burning time. The initial tritium to deuterium ratio $x = 0.0112$. The initial helium-3 to deuterium ratio $y = 0.0399$. The density of the initial pellet $\rho_0 = 5000 \text{ g/cm}^3$. The areal density $\rho_0 R_0 = 12.5 \text{ g/cm}^2$, and the initial temperature of ions and electrons are $T_i(0) = T_e(0) = 10 \text{ keV}$.

ratio of tritium to deuterium particle number in the initial pellet. Figure 2 shows that energy gain is maximum when $y = 0.0399$. As a result, the new configuration $\text{DT}_{x=0.0112} \text{}^3\text{He}_{y=0.0399}$ has higher energy gain than the earlier configuration $\text{DT}_{x=0.0112}$ (table 1). The increase in ${}^3\text{He}$ initial ratio decreases the initial amount of deuterium and tritium. Therefore, we will expect that neutron generation is decreased in this new configuration. Figures 3 and 4 show that after the fuel pellet burns up, the final amounts of tritium and helium-3 are greater than the initial amounts. Thus, we do not need external breeding of tritium and helium-3 when we use this new configuration.

Figure 5 shows ion, electron and radiation temperatures vs. burning time in the $\text{DT}_{x=0.0112} \text{}^3\text{He}_{y=0.0399}$ fuel pellet. This figure shows that ion temperature exceeds at 200 keV. Thus verification deal with reacting particles energy that has been discussed in §2.3 seems to be necessary to calculate fuel pellet parameters. Ion temperature also is higher than electron temperature, because of the bremsstrahlung and inverse Compton effect losses by electrons. Therefore, the ion–electron collision term would play a very important role in the dynamics of these plasmas.

4. Conclusion

In this paper we have analysed the catalytic regime of tritium and helium-3 in deuterium–deuterium fusion fuel pellet, simultaneously. We obtained a new fuel configuration as $\text{DT}_{x=0.0112} \text{}^3\text{He}_{y=0.0399}$. In table 1 we compare this configuration with the one suggested by Eliezer *et al* [11]. As can be seen in table 1, maximum

temperatures, gain and burn fractions of the new fuel ($DT_{x=0.0112} {}^3\text{He}_{y=0.0399}$) is higher than the $DT_{x=0.0112}$ fuel used by Eliezer *et al.* Furthermore, in this new fuel configuration the neutron generation will be reduced by adding ${}^3\text{He}$. This fuel pellet does not require external tritium and helium-3 breeding, because after burn up of fusion fuel pellet the amounts of these ions are equal to or larger than the initial amounts.

References

- [1] S Glasstone and R H Loberg, *Controlled thermonuclear reactions*, Report (E Krieger Publishers, New York, USA, 1975)
- [2] R Feldbacher, *Alternate energy physics program datalib*, Rep. INDC (AUS)-12/G (Technical Univ. of Graz, 1987)
- [3] J M Martinez-Val, G Velarde and Y Ronen, *Nuclear fusion by inertial confinement* (CRC Press, Boca Raton, FL, 1993) Ch. 1
- [4] A A Harms and M Heindler, *Nuclear energy synergetics* (Plenum Press, New York and London, 1982)
- [5] J M Dawson, *CTR Using the P-B11 Reaction*, Rep. PPG-273 (Univ. of California, 1976)
- [6] J M Dawson, *Fusion* (Academic Press, New York, 1981) Vol. 1, Part B, Ch. 16
- [7] S Eliezer, Z Henis and J M Martinez-Val, *Nucl. Fusion* **37**, 985 (1997)
- [8] N A Tahir and D H H Hoffmann, *Fusion Technol.* **33**, 164 (1998)
- [9] S Eliezer, Z Henis, J M Martinez-Val and M Piera, *Phys. Lett.* **A243**, 311 (1998)
- [10] J M Martinez-Val, S Eliezer, Z Henis and M Piera, *Nucl. Fusion* **38**, 1651 (1998)
- [11] S Eliezer, Z Henis, J M Martinez-Val and I Vorbeichik, *Nucl. Fusion* **40**, 195 (2000)
- [12] J S Lewis, *Space Power* **10**, 363 (1991)
- [13] L Wittenberg, J F Santarius and G L Kulcinski, *Fusion Technol.* **10**, 167 (1986)
- [14] J J Duderstadt and G Moses, *Inertial confinement fusion* (Wiley, New York, 1981)
- [15] S Yu Guskov and V B Rosanov, *Nuclear fusion by inertial confinement* edited by G Velarde *et al* (CRC Press, Boca Raton, FL, 1993) Ch. 12
- [16] K A Brueckner and S Jorna, *Rev. Mod. Phys.* **46**, 325 (1974)
- [17] H S Bosch and G M Hale, *Nucl. Fusion* **32**, 611 (1992)
- [18] J D Huba, *NRL Plasma Formulary* (Naval Research Lab., Washington, 2006) p. 35
- [19] G Velarde *et al*, *Laser Part. Beams* **4**, 349 (1986)
- [20] N A Tahir and L A Long, *Nucl. Fusion* **23**, 887 (1983)
- [21] J M Martinez-Val, S Eliezer and M Piera, *Laser Part. Beams* **12**, 681 (1994)
- [22] D J Sigmar and G Joyce, *Nucl. Fusion* **11**, 44756 (1971)
- [23] K Ghosh and S V G Menon, *Nucl. Fusion* **47**, 1176 (2007)
- [24] C K Li and R D Petrasso, *Phys. Rev. Lett.* **70**, 305962 (1993)
- [25] A Gsponer and J P Hurni, *Phys. Lett.* **A253**, 119 (1999)
- [26] G S Fraley, *Phys. Fluids* **17**, 474 (1974)
- [27] G C Pomraning, *The equations of radiation hydrodynamics* (Pergamon Press, Oxford, 1973)
- [28] D C Kershaw, M K Prasad and J D Beason, *J. Quant. Spectrosc. Radiat. Transfer* **36**, 4 (1986)
- [29] S J Rose, *J. Quant. Spectrosc. Radiat. Transfer* **55**, 707 (1996)
- [30] Ya B Zel'dovich and Yu P Raiser, *Physics of shock waves and high-temperature hydrodynamic phenomena* (Academic Press, New York, 1996)
- [31] R Weymann, *Phys. Fluids* **8**, 2112 (1965)